Probing the Star Formation and Metal Enrichment History of the Bulge of M31

Denis Leahy[1]
1. Dept. Physics and Astronomy, University of Calgary

Introduction

M31 is our closest neighboring large galaxy and is a spiral similar in many ways to the Milky Way. Studies of large numbers of stars have been done in detail for our own Galaxy but have uncertainties related often to uncertain distances or to strong extinction. The advantage of studying objects in M31 isthat it is at a well-known distance.

Many surveys have been performed on M31. The previous NUV/FUV survey of M31 was performed by Galex at a spatial resolution of 4 to 5 arcseconds (Kang et al., 2009). The Ultraviolet Imaging Telescope (UVIT) has a spatial resolution of 1 arcsecond and field of view of 28 arcminutes. A comparison between the Galex (left) and UVIT (right) images is shown below.

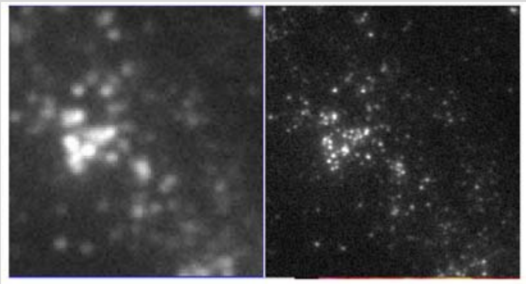

From 2016 to 2019, it surveyed M31 in 19 fields (shown on DSS2 image of M31 below). All UVIT fields have data in the FUV 148 nm filter

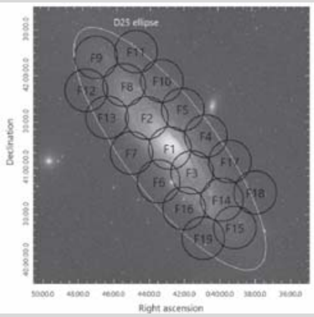

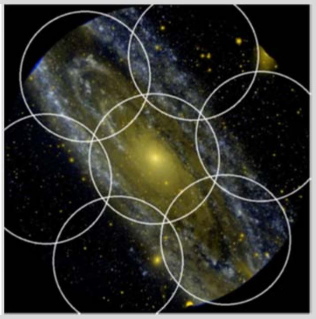

Previous work with UVIT on M31 carried out SED fits for 30 hot stars with PHAT data in the bulge (Leahy et al. 2018), created a UVIT catalog (Leahy et al. 2020a), and matched UVIT with Chandra sources for SED fitting. Some important results are: the bulge of M31 has a hot star populations (5- 20 Msun) which were formed less than ~100 Myr ago; the UVIT sources that are X-ray emitters (see Figure, above right) are mostly globular clusters in M31, with the X-rays from accreting LMXBs and the UV from hot blue-horizontal branch stars;

M31

M31's inner spheroid is primarily composed of red metal-rich stellar populations with broad red giant branches indicative of a **spread in metallicity and stellar age** (e.g. Durrell, Harris, and Pritchet 2004).

Spectroscopic studies revealed a wealth of **substructure and significant inhomogeneity in M31's stellar halo** (e.g Richardson et al. 2009) and a **massive, metal-rich, extended disk** (Ibata et al. 2005).

McConnachie et al. (2018) estimated that the various distinct substructures in M31's stellar halo were produced by **at least 5 separate accretion events within the last 4 Gyr**.

Evidence for **a global burst of star formation 2-4 Gyr ago** (Williams et al. 2015).

Measurements of [Fe/H] and [alpha/Fe] for 129 RGB stars in **the stellar halo of M31**, including its Giant Stellar Stream (Escala+2020) find a low [alpha/Fe] component **consistent with an accretion origin**

Analysis

The spatial structure of the stellar bulge is being measured in NUV and FUV (contour map of central kpc of the M31 shown below left). FUV color- NUV color diagram shown below right, with simple model colors.

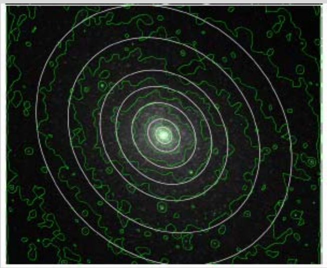

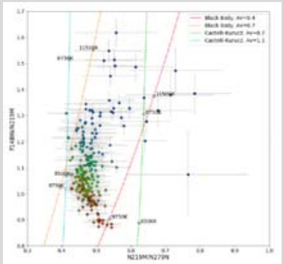

Stellar Population Analysis I (CIGALE)

Extract FUV, NUV, optical, NIR, FIR (17 bands) magnitudes for the bulge, defined by an ellipse with semi-major axis of 188".

The large ellipse was sub-divided into 10 annuli (40 quadrants) of equal-area to study spatial variations

Table 1. Overview of Data Used

Instrument	Filter	Wavelength (μm)
UVIT	F148W	0.1481
UVIT	F169M	0.1608
UVIT	F172M	0.1717
UVIT	N219M	0.2196
UVIT	N279N	0.2792
SDSS	u	0.3543
SDSS	g	0.4770
SDSS	r	0.6231
SDSS	i	0.7625
SDSS	z	0.9134
IRAC	Channel 1	3.6
IRAC	Channel 2	4.5
PACS	Blue	70
PACS	Red	160
SPIRE	PSW	250
SPIRE	PMW	350
SPIRE	PLW	500

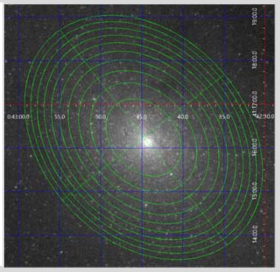

Cigale Analysis

The multiband photometry is modeled using the public CIGALE code (Burgarella et al 2005, Boquien et al, 2019)

CIGALE includes stellar emission, nebular emission, dust emission, dust attenuation

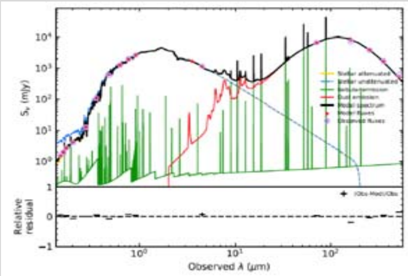

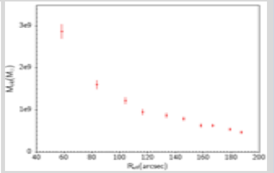

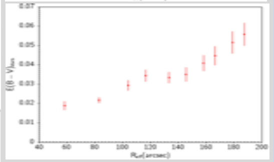

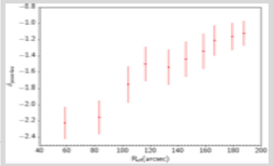

Table 3. M31 Bulge CIGALE Parameters Consistent with Constant

Input Parameter	Mean	Mean Error	Standard Deviation
$E(B-V)_{factor}$	0.382	0.120	0.041
α_{dust}	1.952	0.052	0.041
age_{main} (Myr)	12170	772	120
Tau_{main} (Myr)	446	81	2.6
age_{burst} (Myr)	602	107	57
Tau_{burst} (Myr)	24.9	11.1	0.25
f_{burst}	0.0030	0.0011	0.0006
Z	0.020^a	$8\times10^{-5\ a}$	$1\times10^{-6\ a}$
Derived Parameter	**Mean**	**Mean Error**	**Standard Deviation**
M/L ($M_\odot/L_\odot$)	1.90	0.15	0.04

Table 6. 3-SSP Best-Fit Parameters[a] for the M31 Bulge UV to NIR Data

Region[a]	R_{out} ($''$)	χ^2	M_1^b / M_3^b ($M_\odot$)	age_1 / age_3 (yr)	$\log(Z_1/Z_\odot)$ / $\log(Z_3/Z_\odot)$	$E(B-V)_{1,2}$ / $E(B-V)_3$	M_2^b ($M_\odot$)	age_2 (yr)	$\log(Z_2/Z_\odot)$
Ann1	58.4	8.5E4	7.6E9	1.0E10	0.30	0.18	2.4E8	6.3E8	-0.02
			1.1E4	1.4E7	-0.50	0.10			
Ann2	83.4	6.5E4	4.1E9	1.0E10	0.30	0.18	1.4E8	6.3E8	-0.01
			3.0E3	2.4E7	-0.79	0.22			
Ann3	104.2	5.9E4	3.1E9	1.0E10	0.22	0.21	1.2E8	6.1E8	0.03
			2.0E3	2.6E7	-0.75	0.24			
Ann4	116.7	5.5E4	2.7E9	1.0E10	0.30	0.19	9.5E7	6.1E8	0.03
			1.8E3	2.7E7	-0.76	0.25			

Stellar Population Analysis II (multiple SSPs)

i) include more than 2 SSPs

ii) allow each SSP to have its own metallicity and extinction

Write our own modelling/fitting code using existing SSP models.

Simplifying assumptions: no nebular or dust emission.

Summary of M31 Bulge SFH Analysis

Using CIGALE and our multiple-SSP modelling code, we measure the star formation history and metallicity of the bulge of M31. Ages of old and intermediate age SSP better determined by CIGALE, metallicities and extinction better determined by our code. Compare results to those from Dong+2018, Dong+2015, Saglia+2018, etc. to derive a consistent picture

The bulge has 3 stellar components: -a dominant 12 Gyr old population ([Z/H]=0.3),
-a small (~1% by mass) 700 Myr old population ([Z/H]=0),
-in the central 100", a small (~10^{-6} by mass) ~25 Myr old population ([Z/H]=-0.7).
The metallicity decreases as the stellar populations are younger (agrees with Dong+2018)
This is surprising, but can be explained by the merger history of M31, where the newer populations form from more pristine infalling gas.

This work funded by the Canadian Space Agency

Boquien, M., Burgarella, D., Roehlly, Y., et al. 2019, A&A, 718 622,
Burgarella, D., Buat, V., & Iglesias-Paramo, J. 2005, 724 MNRAS, 360, 1413
Dong, H., Olsen, K., Lauer, T., et al. 2018, MNRAS, 478, 5379
Johnson, L. C., Seth, A. C., Dalcanton, J. J., et al. 2015, ApJ, 802, 127
Kang, Y., Bianchi, L., & Rey, S.-C. 2009, ApJ, 703, 614
Leahy, D., Bianchi, L. & Postma, J. 2018, ApJ, 159, 269
Leahy, D. A. & Chen, Y. 2020, ApJS, 250, 23
Leahy, D. A., Postma, J., Chen, Y., et al. 2020a, ApJS, 247, 47
Leahy, D., Buick, M., Postma, J., et al. 2021, AJ, 161, 215.
Leahy, D., Morgan, C., Postma, J., et al. 2021,768 IJAA, 11, 769 151.
Williams, B. F., Lang, D., Dalcanton, J. J., et al. 2014, ApJS, 215, 9
Postma, J. E., & Leahy, D. 2017, PASP, 129, 115002
Postma, J.E., & Leahy, D. 2020, PASP, 132, 05403 Tandon, S. N., Postma, J., Joseph, P. et al. 2020, AJ, 159, 158
Saglia, R. P., Opitsch, M., Fabricius, M. H., et al. 2018, 796 A&A, 618, A156.